13

Numerical Modeling of Cross-Flow Tube Heat Exchangers with Complex Flow Arrangements

Dawid Taler[1], Marcin Trojan[2] and Jan Taler[2]
[1]*Cracow University of Science and Technology (AGH),*
Department of Energy Systems and Environment Protection,
Faculty of Mechanical Engineering and Robotics,
[2]*Cracow University of Technology,*
Chair of Power Plant Machinery,
Faculty of Mechanical Engineering,
Poland

1. Introduction

Cross-flow tube heat exchangers find many practical applications. An example of such an exchanger is a steam superheater, where steam flows inside the tubes while heating flue gas flows across the tube bundles. The mathematical derivation of an expression for the mean temperature difference becomes quite complex for multi-pass cross-flow heat exchangers with many tube rows and complex flow arrangement (Hewitt et al., 1994; Kröger, 2004; Rayaprolu, 2009; Stultz et al., 1992 ; Taler, 2009a). When calculating the heat transfer rate, the usual procedure is to modify the simple counter-flow LMTD (Logarithmic Mean Temperature Difference) method by a correction F_T determined for a particular arrangement. The heat flow rate $\dot{Q}$ transferred from the hot to cool fluid is the product of the overall heat transfer coefficient U_A, heat transfer area A, correction factor F_T and logarithmic mean temperature difference ΔT_{lm}. The heat transfer equation then takes the form:

$$\dot{Q} = U_A \, A \, F_T \, \Delta T_{lm} \tag{1}$$

However, to calculate steam, flue gas and wall temperature distributions, a numerical model of the superheater is indispensable. Superheaters are tube bundles that attain the highest temperatures in a boiler and consequently require the greatest care in the design and operation. The complex superheater tube arrangements permit an economic trade-off between material unit costs and surface area required to obtain the prescribed steam outlet temperature. Very often, various alloy steels are used for each pass in modern boilers.

High temperature heat exchangers like steam superheaters are difficult to model since the tubes receive energy from the flue gas by two heat transfer modes: convection and radiation. The division of superheaters into two types: convection and radiant superheaters is based on the mode of heat transfer that is predominant. In convection superheaters, the portion of heat transfer by radiation from the flue gas is small. A radiant superheater absorbs heat primarily by thermal radiation from the flue gas with little convective heat flow rate. The share of convection in the total heat exchange of platen superheaters located directly over the combustion chamber amounts only to 10 to 15%. In convective superheaters, the share of radiation heat exchange is lower, but cannot be neglected.

Correct determination of the heat flux absorbed through the boiler heating surfaces is very difficult. This results, on the one hand, from the complexity of heat transfer by radiation of flue gas with a high content of solid ash particles, and on the other hand, from fouling of heating surfaces by slag and ash (Taler et al., 2009b). The degree of the slag and ash deposition is hard to assess, both at the design stage and during the boiler operation. In consequence, the proper size of superheaters can be adjusted only after boiler's start-up. In cases when the temperature of superheated steam at the exit from the superheater stage under examination is higher than its design value, then the area of the surface of this stage has to be decreased. However, if the exit temperature of the steam is below the desired value, then the surface area is increased.

2. Mathematical model of the superheater

To study the impact of superheater fouling on flue gas and steam temperatures, a numerical model of the entire superheater, has been developed. It was assumed that the outer tube surfaces are covered with bonded ash deposits with a uniform thickness. The temperature of the flue gas, tube walls, and steam was determined using the finite volume method (FVM) (Taler, 2009a). The subsequent stages of the superheater were modeled as either cross-parallel-flow or cross-counter-flow. As an example, a numerical model of the first stage convective will be presented in detail (Figs. 1 and 2). The first stage convective superheater is a pendant twelve-pass heat exchanger.

The superheater is constructed of circular bare tubes and is situated at the back of the second and third stages of the superheater (Figs. 1 and 2). The tube is made of grade St 20 carbon steel, having a 42 mm outside diameter and 5mm thick wall. The superheated steam and the combustion products flow at right angles to each other. The convective superheater considered in the paper can be classified according to flow arrangement as a mixed-cross-flow heat exchanger (Figs. 2 and 3). Each individual pass consists of two tubes through which superheated steam flows parallel (Fig. 2).

Based on the energy conservation principle, a mathematical model of steam superheater with 12 tube rows and complex flow arrangement was developed.

The radiant and convective superheaters are located in boiler passes through which high temperature flue gas flows. The gas temperature drops from about 1100 ˚C at the exit of the furnace chamber to about 400 ˚C before entering the economizer. Radiant platen superheaters are located in areas of highest flue gas temperature and the water heater in the lowest temperature pass.

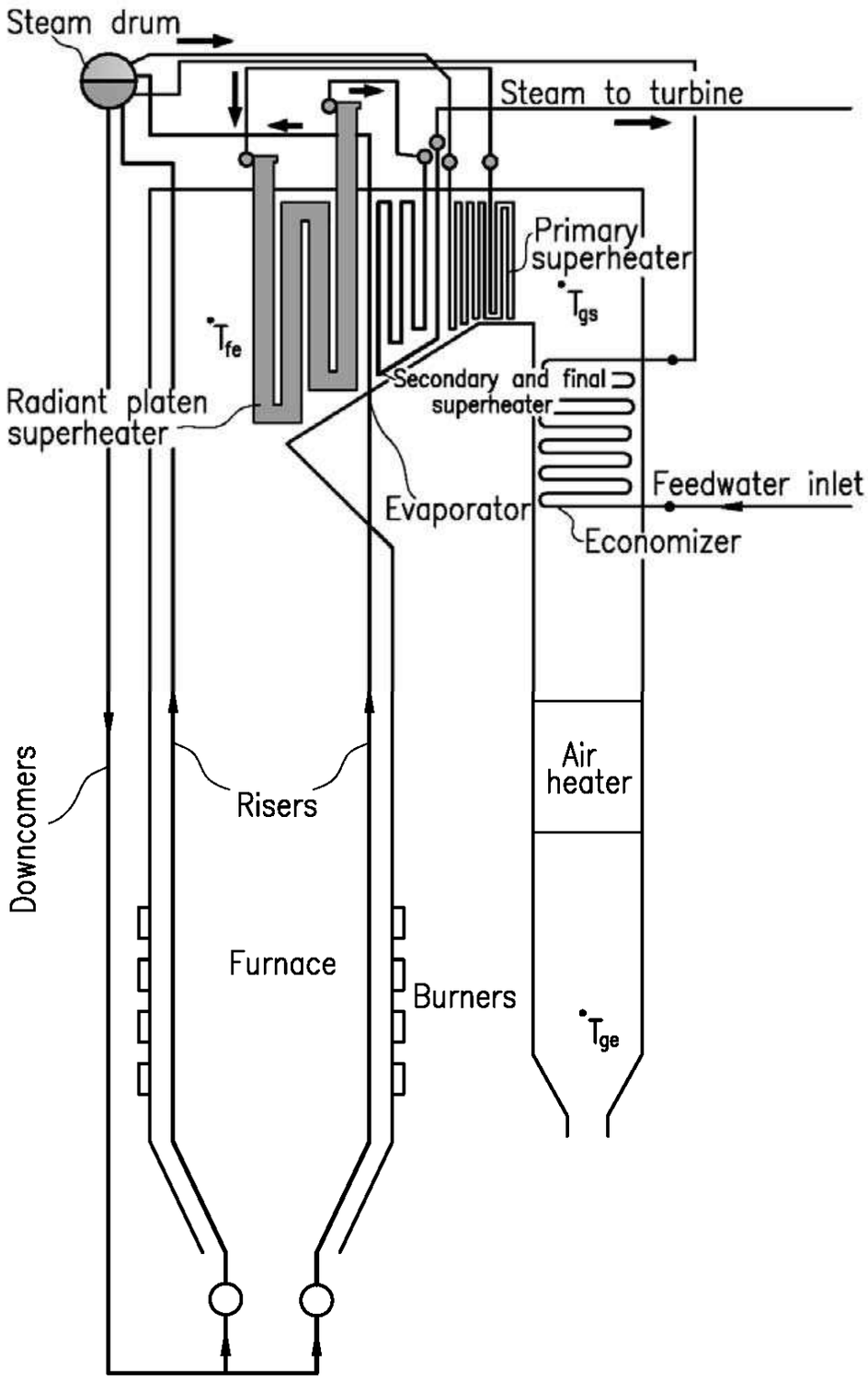

Fig. 1. 50 MW coal-fired utility boiler with steam flow rate of $210 \cdot 10^3$ kg/h: T_{fe}, T_{gs}, and T_{ge} denote flue gas temperatures at the furnace exit, after the superheaters and after the air heater, respectively.

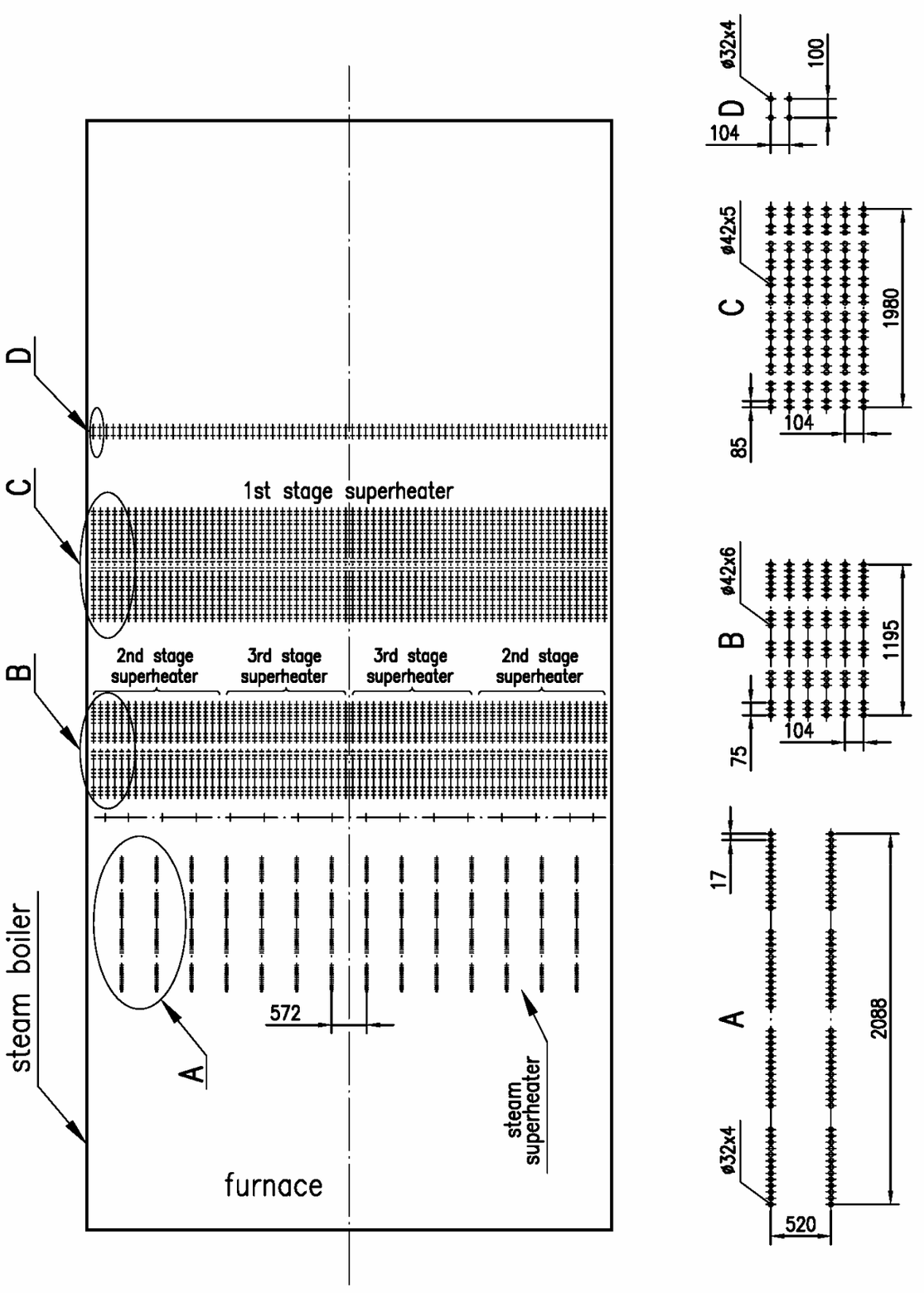

Fig. 2. Arrangement of boiler heating surfaces.

3. Mathematical model of one row tube heat exchanger

A mathematical model of the cross flow tubular heat exchanger, in which air or flue gas flows transversally through a row of tubes will be developed. The system of partial differential equations describing the space and time changes of water or steam T_1, tube wall T_w, and air or flue gas T_2 temperatures are:

$$\tau_1 \frac{\partial T_1}{\partial t} + \frac{1}{N_1} \frac{\partial T_1}{\partial x^+} = -\left(T_1 - T_w \Big|_{r=r_{in}} \right), \tag{2}$$

$$c_w \rho_w \frac{\partial T_w}{\partial t} = \frac{1}{r} \frac{\partial}{\partial r} \left(r k_w \frac{\partial T_w}{\partial r} \right), \tag{3}$$

$$\tau_2 \frac{\partial T_2}{\partial t} + \frac{1}{N_2} \frac{\partial T_2}{\partial y^+} = -\left(T_2 - T_w \Big|_{r=r_o} \right). \tag{4}$$

The energy balance Equations (2-4) are subject to boundary and initial conditions. The boundary conditions are as follows:

$$T_1\left(x^+, t \right)\Big|_{x^+=0} = f_1(t), \tag{5}$$

$$\left(k_w \frac{\partial T_w}{\partial r} \right)\Big|_{r=r_{in}} = h_1 \left(T_w \Big|_{r=r_{in}} - T_1 \right), \tag{6}$$

$$\left(k_w \frac{\partial T_w}{\partial r} \right)\Big|_{r=r_o} = h_2 \left(T_{m2} - T_w \Big|_{r=r_o} \right), \tag{7}$$

$$T_2\left(y^+, t \right)\Big|_{y^+=0} = f_2(t). \tag{8}$$

The initial conditions are:

$$T_1\left(x^+, t \right)\Big|_{t=0} = T_{1,0}\left(x^+ \right), \tag{9}$$

$$T_w\left(x^+, r, t \right)\Big|_{t=0} = T_{w,0}\left(x^+, r \right), \tag{10}$$

$$T_2\left(x^+, y^+, t \right)\Big|_{t=0} = T_{2,0}\left(x^+, y^+ \right). \tag{11}$$

The symbols $f_1(t)$ and $f_2(t)$ denote functions describing the variation of the boundary temperatures of fluids in time. The symbol T_{m2} stands for the mean gas temperature over the row thickness defined as:

$$T_{m2} = \int_0^1 T_2\left(x^+, y^+, t \right) dy^+. \tag{12}$$

The numbers of heat transfer units N_1 and N_2 are given by:

$$N_1 = \frac{h_1 A_{in}}{\dot{m}_1 c_{p1}}, N_2 = \frac{h_2 A_o}{\dot{m}_2 c_{p2}}, \tag{13}$$

where:

$$A_{in} = U_{in} L_x, \quad A_o = U_o L_x.$$

The time constants τ_1, τ_w, τ_f, and τ_2 are:

$$\tau_1 = \frac{m_1 c_{p1}}{h_1 A_{in}}, \quad \tau_w = \frac{m_w c_w}{h_1 A_{in} + h_2 A_o}, \quad \tau_2 = \frac{m_2 c_{p2}}{h_2 A_o}, \tag{14}$$

where:

$$m_1 = A_{in} L_x \rho_1, \; m_2 = \left(s_1 s_2 - \frac{\pi d_o^2}{4} \right) L_x \rho_2, \; m_w = U_m \delta_w L_x \rho_w, \; U_m = \left(U_{in} + U_o \right) / 2.$$

The transient fluids and wall temperature distributions in one row heat exchanger (Fig. 3) are then determined by the explicit finite difference method.

3.1 Transient model of one row tube heat exchanger

Transient distributions of fluid and tube wall temperatures were determined using an explicit finite-difference method. The tube wall was divided into three control volumes (Fig. 3). The finite difference cell is shown in Fig. 3.

Approximating Eq.(2) using the explicit finite difference method gives:

$$T_{1,i+1}^{n+1} = T_{1,i+1}^{n} - \frac{\Delta t}{N_{1,i}^{n} \tau_{1,i}^{n}} \frac{T_{1,i+1}^{n} - T_{1,i}^{n}}{\Delta x^{+}} - \frac{\Delta t}{\tau_{1,i}^{n}} \left(\frac{T_{1,i}^{n} + T_{1,i+1}^{n}}{2} - T_{ww,i}^{n} \right), \quad i = 1,...,N, \quad n = 0,1,... \; . \tag{15}$$

The finite volume method (Taler, 2009a) was used to solve Eq.(3). The ordinary differential equations for wall temperatures at nodes were solved using the explicit Euler method to obtain:

$$T_{ww,i}^{n+1} = T_{ww,i}^{n} + \alpha \left(T_{wm,i}^{n} \right) \times$$
$$\times \Delta t \left\{ \frac{r_2}{r_w} \frac{T_{wm,i}^{n} - T_{ww,i}^{n}}{\left(\Delta r \right)^2} + \frac{r_0}{r_w} \frac{T_{wm,i}^{n} - \left[\left(2 h_1^{n} \cdot \Delta r \right) / k \left(T_{wm,i}^{n} \right) \right] \left(T_{ww,i}^{n} - \frac{T_{1,i}^{n} + T_{1,i+1}^{n}}{2} \right) - T_{ww,i}^{n}}{\left(\Delta r \right)^2} \right\} \tag{16}$$

$$T_{wm,i}^{n+1} = T_{wm,i}^{n} + \alpha \left(T_{wm,i}^{n} \right) \Delta t \left[\frac{2 r_3}{r_2 + r_3} \cdot \frac{T_{wz,i}^{n} - T_{wm,i}^{n}}{\left(\Delta r \right)^2} + \frac{2 r_2}{r_2 + r_3} \frac{T_{ww,i}^{n} - T_{wm,i}^{n}}{\left(\Delta r \right)^2} \right] \tag{17}$$

$$T_{wz,i}^{n+1} = T_{wz,i}^{n} + \alpha\left(T_{wm,i}^{n}\right)\times$$

$$\times\Delta t\left\{\frac{r_5}{r_z}\frac{T_{wm,i}^{n}+\left[\left(2h_2^n\cdot\Delta r\right)/k\left(T_{wm,i}^{n}\right)\right]\left[\frac{\left(T_{2,i}^{'}\right)^n+\left(T_{2,i}^{''}\right)^n}{2}-T_{wz,i}^{n}\right]-T_{wz,i}^{n}}{\left(\Delta r\right)^2}+\frac{r_3}{r_z}\frac{T_{wm,i}^{n}-T_{wz,i}^{n}}{\left(\Delta r\right)^2}\right\} \quad (18)$$

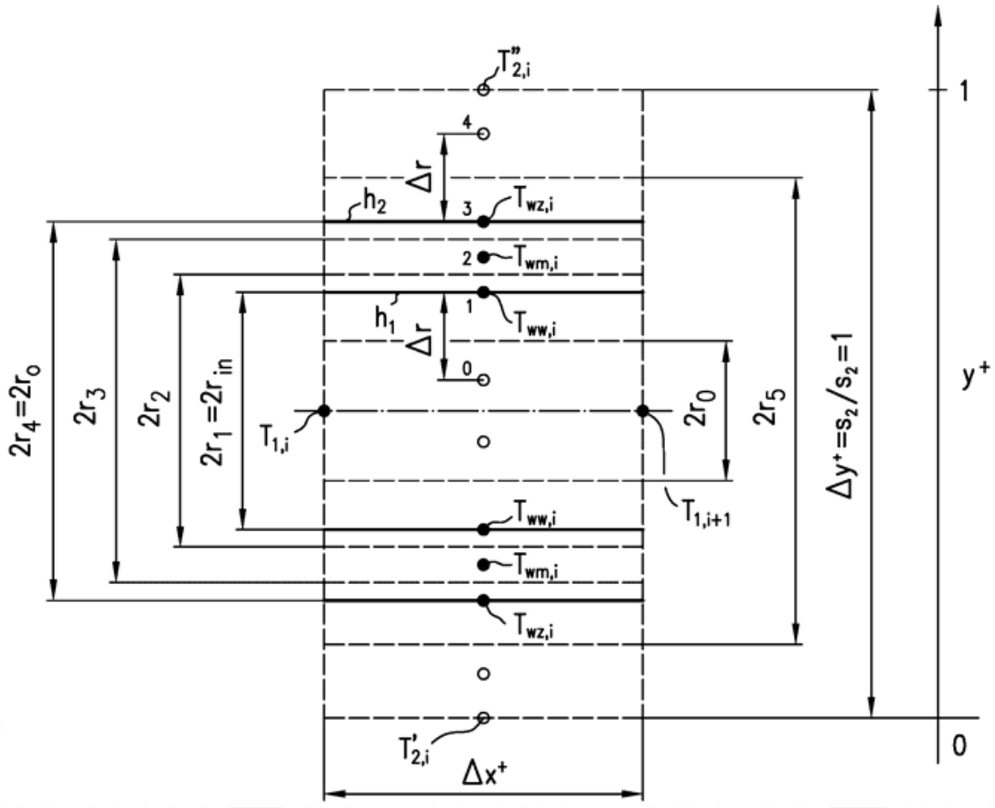

Fig. 3. Control volume for one-row cross-flow tube heat exchanger.

Solving Eq. (4) using the explicit Euler method gives the temperature of the fluid 2 at the exit of the finite volume (Fig.3):

$$\left(T_{2,i}^{''}\right)^{n+1} = \left(T_{2,i}^{''}\right)^{n} + \frac{\Delta t}{N_{2,i}^{n}\tau_{2,i}^{n}}\left[\left(T_{2,i}^{'}\right)^{n}-\left(T_{2,i}^{''}\right)^{n}\right]+\frac{\Delta t}{\tau_{2,i}^{n}}\left[T_{wz,i}^{n}-\frac{\left(T_{2,i}^{'}\right)^{n}+\left(T_{2,i}^{''}\right)^{n}}{2}\right],$$

$$i = 1,\ldots,N\ ,\ n = 0,1,\ldots\ . \quad (19)$$

The initial temperature distributions for the fluid 1 and 2 are given by Equations (9-11), which can be written as:

$$T_{ww,i}\big|_{t=0} = T^0_{ww,i}\,,\quad T_{wm,i}\big|_{t=0} = T^0_{wm,i}\,,\quad T_{wz,i}\big|_{t=0} = T^0_{wz,i}\,,\quad i = 1,...,N\,, \tag{20}$$

where the symbols $T^0_{ww,i}$, $T^0_{wm,i}$, and $T^0_{wz,i}$ denote the wall temperatures at the nodes.
The boundary conditions for fluids are given by Equations (5) and (8). The presented finite difference method is accurate and easy to program. In order to assure the stability of the calculations, the Courant conditions for both fluids and the stability condition for the Fourier equation defining transient heat conduction in the tube wall, should be satisfied.

4. Mathematical model of convective superheater

The flow arrangement and division of the first stage convective superheater into finite volumes is depicted in Fig. 4.
The superheated steam and the combustion products flow at right angles to each other. The first stage of a convective superheater can be classified according to flow arrangement as a mixed-cross-flow heat exchanger. The superheater tubes are arranged in-line (Fig. 5b). Each individual pass consists of two tubes through which superheated steam flows parallel. The tube's outer surface is covered with a layer of ash deposits.
In the following, finite volume heat balance equations will be formulated for the steam, the tube wall, and the flue gas. A steam side energy balance for the ith finite volume gives (Fig. 5a):

$$\dot{m}_s\, c_{ps}\Big|_0^{T_{s,i}} T_{s,i} + \pi\, d_{in}\, \Delta x\, h_s \left(T_{w1,i} - \frac{T_{s,i} + T_{s,i+1}}{2} \right) = \dot{m}_s\, c_{ps}\Big|_0^{T_{s,i+1}} T_{s,i+1}\,, \tag{21}$$

Rearranging Eq. (21) gives

$$\dot{m}_s\, c_{ps}\Big|_{T_{s,i}}^{T_{s,i+1}} \left(T_{s,i+1} - T_{s,i} \right) = \Delta A_{in}\, h_s \left(T_{w1,i} - \frac{T_{s,i} + T_{s,i+1}}{2} \right), \tag{22}$$

where the mesh tube inner surface is

$$\Delta A_{in} = \pi\, d_{in}\, \Delta x \tag{23}$$

The steam average specific heat at constant pressure is given by:

$$c_{ps}\Big|_{T_{s,i}}^{T_{s,i+1}} \approx \frac{c_{ps}\left(T_{s,i}\right) + c_{ps}\left(T_{s,i+1}\right)}{2} = \overline{c}_{ps,i} \tag{24}$$

After rewriting Eq. (22) in the form

$$T_{s,i+1} = \frac{1}{\dot{m}_s\, \overline{c}_{ps,i} + \frac{1}{2} h_s\, \Delta A_{in}} \left[\left(\dot{m}_s\, \overline{c}_{ps,i} - \frac{1}{2} h_s\, \Delta A_{in} \right) T_{s,i} + h_s\, \Delta A_{in}\, T_{w1,i} \right],\quad i = 1,...,N\,, \tag{25}$$

the Gauss-Seidel method can be applied for an iterative solving nonlinear set of algebraic equations (25). Introducing the mesh number of transfer units for the steam:

$$\Delta N_{s,i+\frac{1}{2}} = \frac{h_s\, \Delta A_{in}}{\dot{m}_s\, \overline{c}_{ps,i}} = \frac{2\, h_s\, \Delta A_{in}}{\dot{m}_s \left[c_{ps}\left(T_{s,i}\right) + c_{ps}\left(T_{s,i+1}\right) \right]} \tag{26}$$

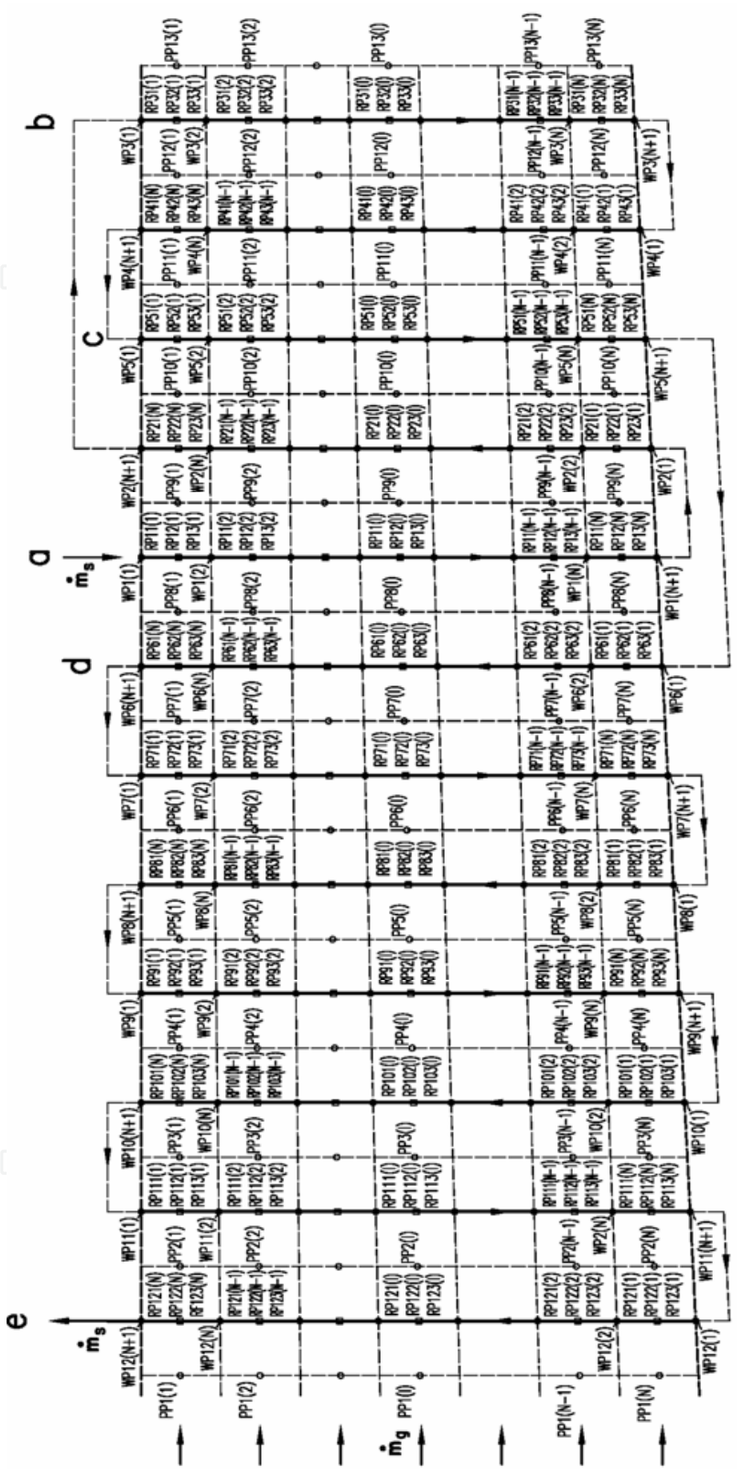

Fig. 4. Superheater flow arrangement and division of superheater into control volumes; o - flue gas, • - water steam, - tube wall; PP1(1),…,PP1(N) – flue gas temperature at the nodes before the superheater, WP1(1),…,WP1(N+1) – steam temperature at the nodes in the first superheater pass.

and dividing Eq. (26) by $\dot{m}_s \bar{c}_{ps,i}$, we have:

$$T_{s,i+1} = \frac{1}{1+\frac{1}{2}\Delta N_{s,i+\frac{1}{2}}}\left[\left(1-\frac{1}{2}\Delta N_{s,i+\frac{1}{2}}\right)T_{s,i} + \Delta N_{s,i+\frac{1}{2}} T_{w1,i}\right], \quad i=1,\ldots,N \tag{27}$$

where: $\Delta x = L_x / N$ - the mesh size, L_x – the tube length.

The energy conservation principle for the flue gas applied for the finite control volume (Fig. 5) is:

$$\Delta\dot{m}_g\, c_{pg}\Big|_0^{T'_{g,i}} T'_{g,i} = \Delta\dot{m}_g\, c_{pg}\Big|_0^{T''_{g,i}} T''_{g,i} + \pi\left(2r_o + 2\delta_z\right)\Delta x\, h_g\left(\frac{T'_{g,i}+T''_{g,i}}{2} - T_{w3,i}\right) \tag{28}$$

After rearranging Eq. (28), we obtain:

$$\Delta\dot{m}_g\, \bar{c}_{pg,i}\left(T'_{g,i} - T''_{g,i}\right) = \Delta A_z\, h_g\left(\frac{T'_{g,i}+T''_{g,i}}{2} - T_{w3,i}\right) \tag{29}$$

where the mesh outer surface of deposits is (Fig. 6):

$$\Delta A_z = \pi\left(2r_o + 2\delta_z\right)\Delta x\ . \tag{30}$$

The flue gas average specific heat at constant pressure is given by:

$$\bar{c}_{pg,i} = \frac{c_{pg}\left(T''_{g,i}\right) + c_{pg}\left(T'_{g,i}\right)}{2}\ . \tag{31}$$

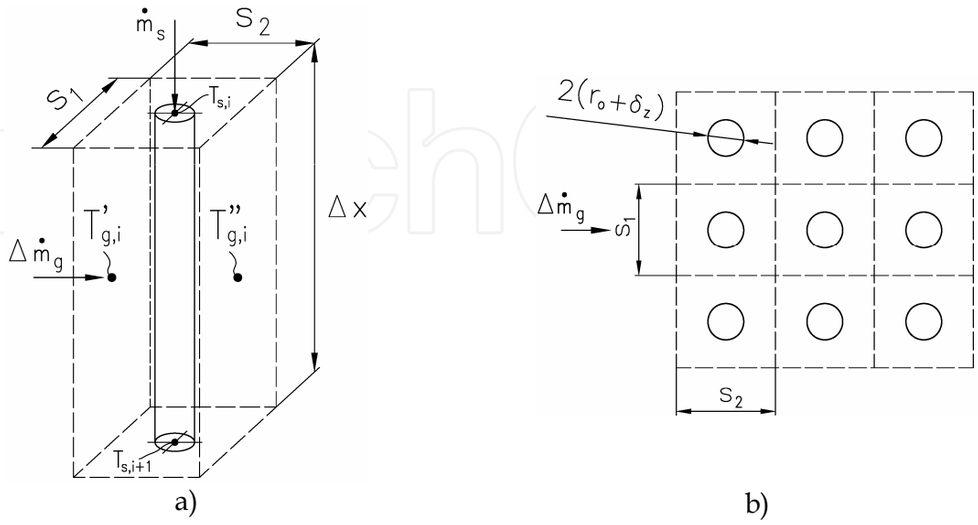

Fig. 5. Finite volume for energy balance on the steam and gas sides (a) and in-line array of superheater tubes (b).

Equation (29) can be written as:

$$T''_{g,i} = \frac{1}{\Delta\dot{m}_g\,\overline{c}_{pg,i} + \frac{1}{2}h_g\,\Delta A_z}\left[\left(\Delta\dot{m}_g\,\overline{c}_{pg,i} - \frac{1}{2}h_g\,\Delta A_z\right)T'_{g,i} + h_g\,\Delta A_z T_{w3,i}\right]. \tag{32}$$

Introducing the mesh number of transfer units for the gas:

$$\Delta N_{g,i+\frac{1}{2}} = \frac{h_g\,\Delta A_z}{\Delta\dot{m}_g\,\overline{c}_{pg,i}} = \frac{2h_g\,\Delta A_z}{\Delta\dot{m}_g\left[c_{pg}\left(T'_{g,i}\right) + c_{pg}\left(T''_{g,i}\right)\right]} \tag{33}$$

and dividing Eq. (33) by $\dot{m}_g\,\overline{c}_{pg,i}$ we obtain:

$$T''_{g,i} = \frac{1}{1 + \frac{1}{2}\Delta N_{g,i+\frac{1}{2}}}\left[\left(1 - \frac{1}{2}\Delta N_{g,i+\frac{1}{2}}\right)T'_{g,i} + \Delta N_{g,i+\frac{1}{2}}\,T_{w3,i}\right], i = 1, \ldots, N. \tag{34}$$

Subsequently, energy conservation equations for the tube wall (Fig. 6) will be written.

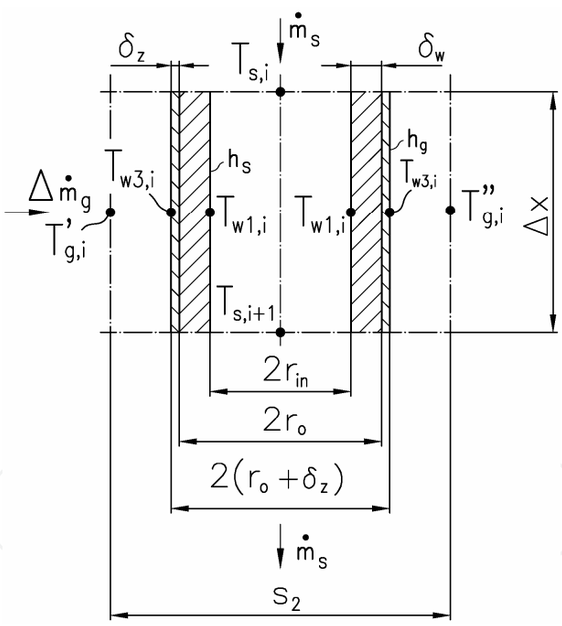

Fig. 6. Tube wall with a layer of deposits at the outer tube surfaces.

The tube wall and the deposit layer are divided into three finite volumes (Fig. 7).
Energy conservation equations may be written as:

node 1

$$h_s\left(\overline{T}_{s,i} - T_{w1,i}\right)\pi\,d_{in} + \frac{k_w\left(T_{w1,i}\right) + k_w\left(T_{w2,i}\right)}{2}\frac{T_{w2,i} - T_{w1,i}}{\delta_w}\pi\,d_c = 0, \tag{35}$$

where: $d_c = \left(d_{in} + d_o\right)/2 = r_{in} + r_o$, $\overline{T}_{s,i} = \dfrac{T_{s,i} + T_{s,i+1}}{2}$.

node 2

$$\frac{k_w\left(T_{w1,i}\right) + k_w\left(T_{w2,i}\right)}{2}\frac{T_{w1,i} - T_{w2,i}}{\delta_w}\pi d_c + k_z\frac{T_{w3,i} - T_{w2,i}}{\delta_z}\pi d_s = 0, \tag{36}$$

where: $d_s = d_o + \delta_z = 2r_o + \delta_z$.

node 3

$$h_g\left(\overline{T}_{g,i} - T_{w3,i}\right)\pi\left(d_o + 2\delta_z\right) + k_z\frac{T_{w2,i} - T_{w3,i}}{\delta_z}\pi d_s = 0. \tag{37}$$

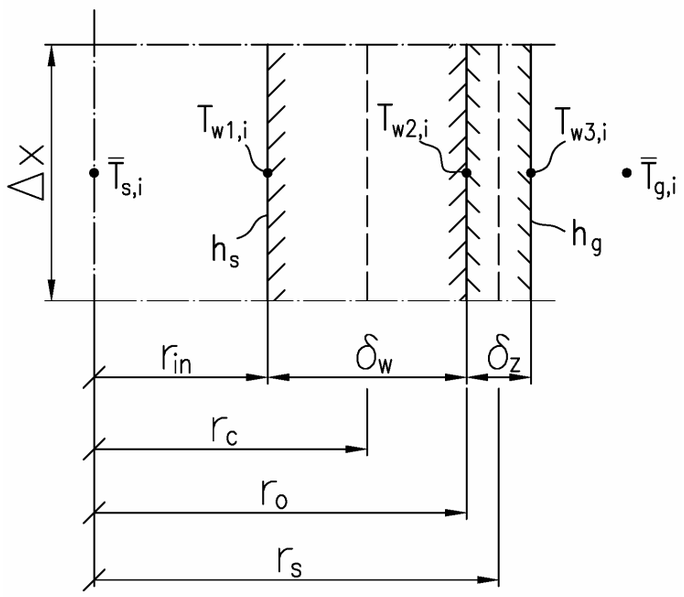

Fig. 7. Division of the tube wall and deposit layer into three control volumes.

Algebraic equations (35) – (37) can be rewritten in a form which is suitable for solving equation sets by using the Gauss – Seidel method:

$$T_{w1,i} = \frac{1}{h_s d_{in} + \dfrac{k_w\left(T_{w1,i}\right) + k_w\left(T_{w2,i}\right)}{2}\dfrac{d_c}{\delta_w}}\left[h_s\overline{T}_{s,i}d_{in} + \frac{k_w\left(T_{w1,i}\right) + k_w\left(T_{w2,i}\right)}{2}\frac{d_c}{\delta_w}T_{w2}\right], \tag{38}$$

$$T_{w2,i} = \frac{1}{\dfrac{k_w\left(T_{w1,i}\right) + k_w\left(T_{w2,i}\right)}{2}\dfrac{d_c}{\delta_w} + \dfrac{k_z}{\delta_z}d_s}\left[\frac{k_w\left(T_{w1,i}\right) + k_w\left(T_{w2,i}\right)}{2}\frac{d_c}{\delta_w}T_{w1,i} + k_z\frac{d_s}{\delta_z}T_{w3,i}\right], \tag{39}$$

$$T_{w3,i} = \frac{1}{\left[h_g \left(d_o + 2\delta_z \right) + k_z \frac{d_s}{\delta_z} \right]} \left[h_g \left(d_o + 2\delta_z \right) \overline{T}_{g,i} + k_z \frac{d_s}{\delta_z} T_{w2,i} \right]. \tag{40}$$

Equations (38) – (40) can be used for building mathematical models of steam superheaters.
To solve Eqs. (27), (34) and (38) – (40) two boundary conditions are prescribed: inlet steam temperature $T_{s,inlet}$ and flue gas temperature $T_{g,inlet}$ before the superheater:

$$WP1(1) = T_{s,inlet} \text{ and } PP1(I) = T_{g,inlet},\ I = 1,...,N \tag{41}$$

5. Convection and radiation heat transfer coefficients

The convective heat transfer coefficient at the tube inner surface h_s and the heat transfer on the flue gas side h_{cg} were calculated using correlations given in (Kuznetsov et al., 1973). The effect of radiation on the heat transfer coefficient h_g is accounted for by adding the radiation heat transfer coefficient h_{rg} (Taler et al., 2009c; Kuznetsov et al., 1973) to the convective heat transfer, e.g. $h_g = h_{cg} + h_{rg}$.
For in-line arrays, in which tubes in successive rows are in-line in the direction of flue gas flow, the following correlation was used for calculating convective heat transfer coefficient h_{cg} (Kuznetsov et al., 1973):

$$Nu_{cg} = 0.2 C_s C_z \mathrm{Re}_g^{0.65} \mathrm{Pr}_g^{0.33}. \tag{42}$$

Similar correlation was used for staggered tube arrays:

$$Nu_{cg} = C_s C_z \mathrm{Re}_g^{0.6} \mathrm{Pr}_g^{0.33} \tag{43}$$

where: $Nu_{cg} = h_{cg}\left(d_o + 2\delta_z\right)/k_g$ - Nusselt number, Re - Reynolds number, Pr - Prandtl number, C_s, C_z - correction factors for tube arrangement and for the effect of number of tube rows in the array, respectively.
The cross flow Reynolds number is given by: $\mathrm{Re} = \rho_g w_{g\max}\left(d_o + \delta_z\right)/\mu_g$, where ρ_g - density, μ_g - dynamic viscosity, $w_{g\max}$ - maximum gas velocity, calculated for the minimum flow area between tubes normal to the local flow direction.
For calculating the heat transfer coefficient on the steam side the well known Dittus – Boelter equation was used:

$$Nu_s = 0.023 \mathrm{Re}_s^{0.8} \mathrm{Pr}_s^{0.33} C_t \tag{44}$$

where: C_t - correction factor for surface-to-bulk physical property variations.
The radiation heat transfer coefficients were also calculated using simple formulas, which are widely applied to the design of boilers and other heating equipment. The Standard Method (Kuznetsov et al., 1973; Kakaç, 1991) applies the following formula:

$$h_{rg} = \sigma \frac{1 + \varepsilon_w}{2} \varepsilon_g \frac{\overline{T}_g^4 - T_w^4}{\overline{T}_g - T_w} \tag{45}$$

where: $\sigma = 5.67 \times 10^{-8}$ W/(m² · K⁴) – Stefan-Boltzmann constant, ε_g , ε_w –gas and tube wall emissivity, respectively, $\overline{T}_g$ - gas mean temperature over tube row, T_w - tube wall temperature.
When solid particles are absent in the gaseous combustion products (gas or oil fired boilers), then the following modified formula (Kuznetsov et al., 1973) is recommended:

$$h_{rg} = \sigma \frac{1+\varepsilon_w}{2} \varepsilon_g \frac{\overline{T}_g^4 - \left(T_w / \overline{T}_g\right)^{3.6} \overline{T}_g^4}{\overline{T}_g - T_w} . \tag{46}$$

The radiation heat transfer coefficient h_{rg} can be calculated using a simple formula derived in (Taler et al., 2009c):

$$h_{rg} = \frac{\sigma \varepsilon_e as}{as + \varepsilon_e} \frac{\left(\overline{T}_g^4 - T_w^4\right)}{\left(\overline{T}_g - T_w\right)} \tag{47}$$

where: a – absorption coefficient, s – geometric mean beam length, $\varepsilon_e = 2\varepsilon_w / (2 - \varepsilon_w)$.
The mean beam length s for in-line and staggered tube arrays is given by:

$$s = C \frac{(d_o + 2\delta_z)}{4} \left(\frac{4}{\pi} \frac{s_1 s_2}{(d_o + 2\delta_z)^2} - 1 \right) \tag{48}$$

where C < 4.0. A value of C = 3.6 works well in many situations (Hewitt et al., 1994; Rayaprolu, 2009; Taler et al., 2009c). The coefficient C is assumed to be between C = 3.4 (Stultz et al., 1992) and C = 3.8 (Brandt, 1985). In cases of lager values of the product as, the value of the coefficient C is lower ($3.4 \le C \le 3.6$).

6. Example of superheater modeling

The calculations are based on the following data: tube's outside diameter, $d_o = 0.042m$, tube's inside diameter, $d_{in} = 0.032m$, inlet flue gas temperature, $T_{g,inlet} = 632.6\ ^oC$, inlet steam temperature, $T_{s,inlet} = 337.7\ ^oC$, steam mass flow rate $\dot{m}_s = 46.2\,kg/s$, mean flue gas velocity in the narrowest cross section, $w_g = 7.19\,m/s$, ash deposition thickness $\delta_z = 0.002\,m$, and thermal conductivity of ash layer $k_z = 0.07\,W/(mK)$.
The thermal conductivity of the tube material is given by the following expression:

$$k_w = 35.54 + 0.004084T - 2.0891 \cdot 10^{-5} T^2 , \tag{49}$$

where the thermal conductivity k_w is in W/(m·K) and temperature T in °C.
Figures 8 and 9 illustrate the predictions of the mathematical model. The calculated steam temperature and mean flue gas temperature behind the superheater are: 400.9 °C and 558.6 °C, respectively. The computed steam temperature increase is: ΔT_s = 400.9-337.7=63.2 K while the measured increase is: $\Delta T_s = 63.3\,K$.
The agreement between the measured and calculated steam temperature rise is very good.

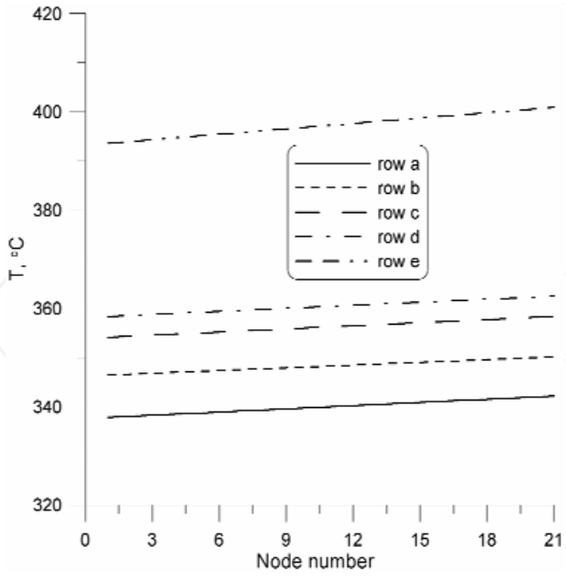

Fig. 8. Steam temperature distribution in selected passes; a, b, c, d, e – symbol of the pass (Fig. 4).

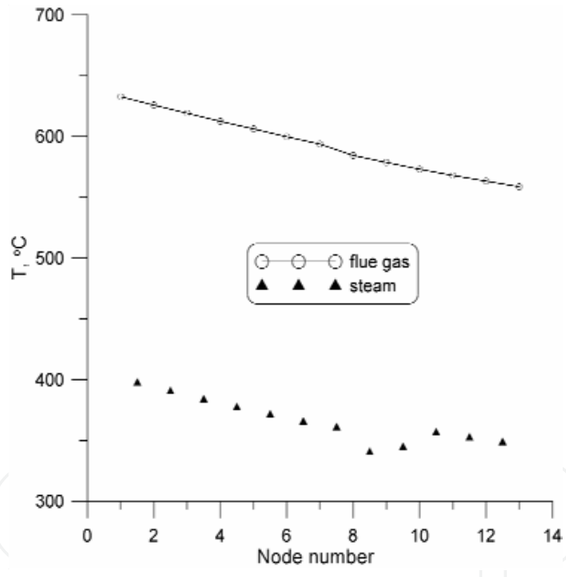

Fig. 9. Flue gas and steam temperature in the middle of superheater in direction of flue gas flow (from the left to the right side of superheater).

The mathematical model of the superheater developed in the paper allows to determine the wall and ash deposits temperature. The tube temperature at the inner and outer surfaces at the inlet of the superheater are $T_{w1,1} = 341.0\,^{o}C$ and $T_{w2,1} = 341.89\,^{o}C$.
The temperature rises significantly over the ash deposit layer since the temperature at the outer surface of the deposit layer is $T_{w3,1} = 522.28\,^{o}C$. Similar results are obtained at the outlet of the superheater: $T_{w1,N+1} = 403.61\,^{o}C$, $T_{w2,N+1} = 404.45\,^{o}C$, and $T_{w3,N+1} = 573.63\,^{o}C$ (Fig. 7).

It can be seen from the inspection of the results that the ash layer has a great influence on the temperature of ash deposit layer. With an increasing ash deposit layer the heat flow rate from the flue gas to the steam decreases since the temperature difference between the flue gas and ash deposit surface drops.

7. Conclusions

Cross-flow tube heat exchangers find many applications in practice. An example of such an exchanger is a steam superheater, where the steam flows inside the tubes while heating flue gas flows across the tube bundles. The mathematical derivation of an expression for the mean temperature difference becomes quite complex for multi-pass cross-flow heat exchangers with many tube rows and complex flow arrangement. When calculating the heat transfer rate, the usual procedure is to modify the simple counter-flow LMTD (Logarithmic Mean Temperature Difference) method by a correction F_T determined for a particular arrangement. The heat flow rate $\dot{Q}$ transferred from the hot to cool fluid is the product of the overall heat transfer coefficient U_A, heat transfer area A, correction factor F_T and logarithmic mean temperature difference ΔT_{lm}. The heat transfer equation then takes the form: $\dot{Q} = U_A \, A \, F_T \, \Delta T_{lm}$. However, to calculate the steam, flue gas and wall temperature distributions, a numerical model of the superheater is indispensable. Superheaters are the tube bundles that attain the highest temperatures in a boiler and consequently require the greatest care in the design and operation. The complex superheater tube arrangements permit the economic trade-off between material unit costs and surface area required to obtain the prescribed steam outlet temperature. Very often, various alloy steels are used for each pass in modern boilers. High temperature heat exchangers, like steam superheaters, are difficult to model since the tubes receive energy from the flue gas by two heat transfer modes: convection and radiation. The division of superheaters into two types: convection and radiant superheaters is based on the mode of heat transfer that is predominant. In convection superheaters, the portion of heat transfer by radiation from the flue gas is small. A radiant superheater absorbs heat primarily by thermal radiation from the flue gas with little convective heat flow rate. The share of convection in the total heat exchange of platen superheaters located directly over the combustion chamber amounts only to 10 to 15%. In convective superheaters, the share of radiation heat exchange is lower, but cannot be neglected. Correct determination of the heat flux absorbed through the boiler heating surfaces is very difficult. This results, on the one hand, from the complexity of heat transfer by radiation of flue gas with a high content of solid ash particles, and on the other hand, from the fouling of heating surfaces by slag and ash. The degree of the slag and ash deposition is hard to assess, both at the design stage and during the boiler operation. In consequence, the proper size of superheaters can be adjusted after taking the boiler into operation. In cases when the temperature of superheated steam at the exit from the superheater stage under examination is higher than design value, then the area of the surface of this stage has to be decreased. However, if the exit temperature of the steam is below the desired value, then the surface area is increased.

To overcome the difficulties mentioned above, the general principles of mathematical modeling of steady-state and unsteady heat transfer in cross-flow tube heat exchangers with complex flow arrangements which allow of the simulation of multipass heat exchangers with many tube rows were presented. The finite volume method (FVM) was used to derive the algebraic equation system for determining flue gas, wall, and steam temperature at the

nodes of the finite volumes. A numerical model of multipass steam superheater with twelve passes was developed. The convection and radiation heat transfer was accounted for on the flue gas side. In addition, the deposit layer was assumed to cover the outer surface of the tubes. The calculation results were compared with the experimental data. The computed steam temperature increase over the entire superheater corresponds very well with the measured steam temperature rise. The developed modeling technique can especially be used for modeling tube heat exchangers when detail information on the tube wall temperature distribution is needed.

8. Symbols

a	- absorption coefficient, 1/m
A	- area, m^2
A_{in} , A_o	- inside and outside cross section area of the tube, m^2
c	- specific heat, J/(kg·K)
$\overline{c}$	- mean specific heat, J/(kg·K)
c_p	- specific heat at constant pressure, J/(kg·K)
F_T	- correction factor for a particular flow arrangement,
h	- heat transfer coefficient, W/(m^2·K)
k	- thermal conductivity, W/(m·K)
L_x	- tube length in the heat exchanger, m
Nu	- Nusselt number
m	- mass, kg
$\dot{m}$	- mass flow rate, kg/s
Pr	- Prandtl number
$\dot{Q}$	- heat flow rate, W
r	- radius, m
Re	- Reynolds number
s_1	- pitch of tubes in plane perpendicular to flow (height of fin), m
s_2	- pitch of tubes in direction of flow, m
t	- time, s
T	- temperature, °C
$T_2^{'}$, $T_2^{''}$	- gas temperature before and after tube row, °C
U	- perimeter, m
U_A	- overall heat transfer coefficient, W/(m^2·K)
U_{in} , U_o	- inner and outer perimeter of the oval tube, respectively, m
w	- fluid velocity, m/s
x, y, z	- Cartesian coordinates
$x^+ = x / L_x$	- dimensionless coordinate
$y^+ = y / s_2$	- dimensionless coordinate

8.1 Greek symbols

$\alpha = k / (c\ \rho)$	- thermal diffusivity, m^2/s
$\Delta \dot{m}_g$	- flue gas mass flow rate through the control volume , kg/s,

ΔT - temperature difference, K
Δx , Δy - control volume size in x and y direction, m
$\Delta x^+ = 1/N$ - dimensionless control volume size
δ - thickness, m,
ε - emissivity,
ρ - density, kg/m^3
τ - time constant, s

8.2 Subscripts

g - flue gas
lm - logarithmic mean
m - mean
r - tube
s - steam
w - wall
in - inner
o - outer
1 - fluid flowing inside the tube
2 - fluid flowing in perpendicular direction to tubes

9. References

Brandt, F. (1985). *Wärmeübertragung in Dampferzeugern und Wärmetauschern*, FDBR-Fachverband Dampfkessel-Behälter- und Rohrleitungsbau, ISBN 3-8027-2535-2 Vulkan-Verlag, Essen

Hewitt G. F., Shires G. L., Bott T.R. (1994). *Process heat transfer*, CRC Press, ISBN 0-8493-9918-1, Boca Raton

Kakaç, S., Boilers (1991). *Evaporators, and Condensers*, Wiley, ISBN 0471621706, New York,

Kröger D. G. (2004). *Air-cooled Heat Exchangers and Cooling Towers*, ISBN 0820603007, Chemical Publishing Company, New York, USA

Kuznetsov N. V., Mitor V.V., Dubovskij I.E., Karasina E.S., Editors (1973). *Standard Methods of Thermal Design for Power Boilers*, Central Boiler and Turbine Institute, Energija, UDK 621 181 001 24 : 536 7 (083 75), Moscow, (in Russian)

Rayaprolu K.(2009). *Boilers for Power and Process*, CRC Press, ISBN 978-14200-7536-6, Boca Raton

Stultz S.C., Kitto J.B., Editors (1992). *Steam. Its Generation and Use*., The Babcock & Wilcox Company, Fortieth edition, ISBN 09634570-0-4, Barberton, Ohio

Taler D. (2009a). *Dynamics of Tube Heat Exchangers*, University of Science Publishing Hous (UNWD AGH), ISSN 0867-6631, Cracow (in Polish)

Taler J., Trojan M., Taler D. (2009b). *Archives of Thermodynamcs*, Vol. 30, No. 2, 59 – 76, ISSN 1231 - 0956

Taler J., Taler D. (2009c). *Heat Transfer Engineering*, 30, 661-669, ISSN 0145-7632

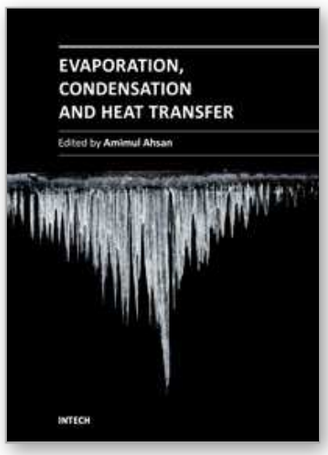

Evaporation, Condensation and Heat transfer
Edited by Dr. Amimul Ahsan

ISBN 978-953-307-583-9
Hard cover, 582 pages
Publisher InTech
Published online 12, September, 2011
Published in print edition September, 2011

The theoretical analysis and modeling of heat and mass transfer rates produced in evaporation and condensation processes are significant issues in a design of wide range of industrial processes and devices. This book includes 25 advanced and revised contributions, and it covers mainly (1) evaporation and boiling, (2) condensation and cooling, (3) heat transfer and exchanger, and (4) fluid and flow. The readers of this book will appreciate the current issues of modeling on evaporation, water vapor condensation, heat transfer and exchanger, and on fluid flow in different aspects. The approaches would be applicable in various industrial purposes as well. The advanced idea and information described here will be fruitful for the readers to find a sustainable solution in an industrialized society.

How to reference
In order to correctly reference this scholarly work, feel free to copy and paste the following:

Dawid Taler, Marcin Trojan and Jan Taler (2011). Numerical Modeling of Cross-Flow Tube Heat Exchangers with Complex Flow Arrangements, Evaporation, Condensation and Heat transfer, Dr. Amimul Ahsan (Ed.), ISBN: 978-953-307-583-9, InTech, Available from: http://www.intechopen.com/books/evaporation-condensation-and-heat-transfer/numerical-modeling-of-cross-flow-tube-heat-exchangers-with-complex-flow-arrangements

INTECH
open science | open minds

InTech Europe
University Campus STeP Ri
Slavka Krautzeka 83/A
51000 Rijeka, Croatia
Phone: +385 (51) 770 447
Fax: +385 (51) 686 166
www.intechopen.com

InTech China
Unit 405, Office Block, Hotel Equatorial Shanghai
No.65, Yan An Road (West), Shanghai, 200040, China
中国上海市延安西路65号上海国际贵都大饭店办公楼405单元
Phone: +86-21-62489820
Fax: +86-21-62489821

IntechOpen